FLOW STRUCTURES AND SEPARATION IN OVEREXPANDED ROCKET NOZZLES

F. Nasuti, M. Onofri
University of Rome "La Sapienza", Rome, Italy

Abstract

The paper analyzes the basic flow structures that may take place inside the nozzle divergent section during the start up and the low altitude flight, when nozzles operate in overexpanded regime. The possible generation of the "inviscid separation phenomenon", and its role on the occurrence of the free- and restricted-shock separation regimes are discussed. On the basis of the analysis of the nozzle behaviour, a semi-analytical model is developed, capable to predict location and shape of the recompression shock, as well as to provide indications on the possible generation of a recirculating flow region behind it, that may yield side loads on the nozzle wall.

Nomenclature

FSS	Free shock separation
M	Mach number
p	Pressure
PR	Nozzle pressure ratio (pc/pa)
RSS	Restricted shock separation
TIC	Truncated ideal contour

Subscripts

a	Ambient condition
c	Chamber condition (or total condition of the incoming flow)
d	Design condition
i	Incoming flow condition
s	Separation condition

Introduction

1.

During the low altitude flight of space launchers and during the engine start-up or shut-down, the nozzles operate in overexpanded regime, and flow separations in the divergent section may take place. In this case, the peculiar flowfield structure may yield side loads on the nozzle wall, with consequent major structural problems.

In the analysis of this phenomenon a milestone contribution was given by Nave and Coffey [1] in 1973. They showed that two possible flow structures may take place in a nozzle with separated flow. The first called Free Shock Separation (FSS) regime, is characterized by a large recirculating region behind the separation point (Fig. 1). In case of asymmetric separation of the boundary layer from the nozzle wall it yields a tilted separation surface, with consequent rise of side loads on the wall. Concerning the second possible flow structure, they observed that downstream of the separation point the flow may reattach to the wall (Fig. 2). Because of the limited extension of this separated region, they called it Restricted Shock Separation (RSS) regime. They also observed that the highest value of side load takes place during the transition from FSS to RSS.

Renewed attention was given to the phenomenon during the development of the Ariane 5 Vulcain engines. The indications of Nave and Coffey were first supported by numerical simulations [2,3] that confirmed the flow transition from FSS to RSS. Then also experiments [4-6] confirmed that the highest values of side loads take place during the transition.

The understanding of the physical causes of this transition has been therefore the main goal of many studies motivated by the request of improvements of the performance of the launcher main engine nozzles.

A common finding of these studies is that the possible generation of vortices and back flow in the core of the divergent section causes the occurrence of RSS [7-10]. In particular, the authors have illustrated [3,10] how this phenomenon is influenced by the geometrical profile of the separation shock that occurs in the overexpanded regime.

According to this explanation, an inviscid mechanism drives the phenomenon. In particular, the driving role is played by the non-uniformity of the flow impinging on the separation shock. Because of this, and because of the downstream quite-uniform pressure, the shock strength cannot be constant along its surface and the shock profile, rather than flat, takes a curved shape.

As shown in Fig. 2, a rotational flow occurs behind the separation shock because of velocity and entropy gradients; it becomes larger for increasing flow non-uniformity upstream, and can thus generate vortical structures. Once a vortex is generated in the center of the divergent section, it represents an obstruction to the main exhausting jet, that deviates towards the wall. As a consequence, a radial flow component is generated that tends to reattach the separated region to the wall, thus switching the flow structure of the separated region from FSS to RSS. Moreover, behind the reattachment point, due to the flow impingement on the wall, a sudden increase of pressure results.

From the nozzle design point of view, in order to reduce the level of side loads, the interest is therefore to understand the relationship between shock structures and vortex generation. In order to achieve a final understanding of these physical mechanisms, a very basic nozzle profile, the Truncated Ideal Contour (TIC), has been considered. Indeed, this nozzle does not feature any oblique internal shock and thus the above phenomena are easier to be analyzed.

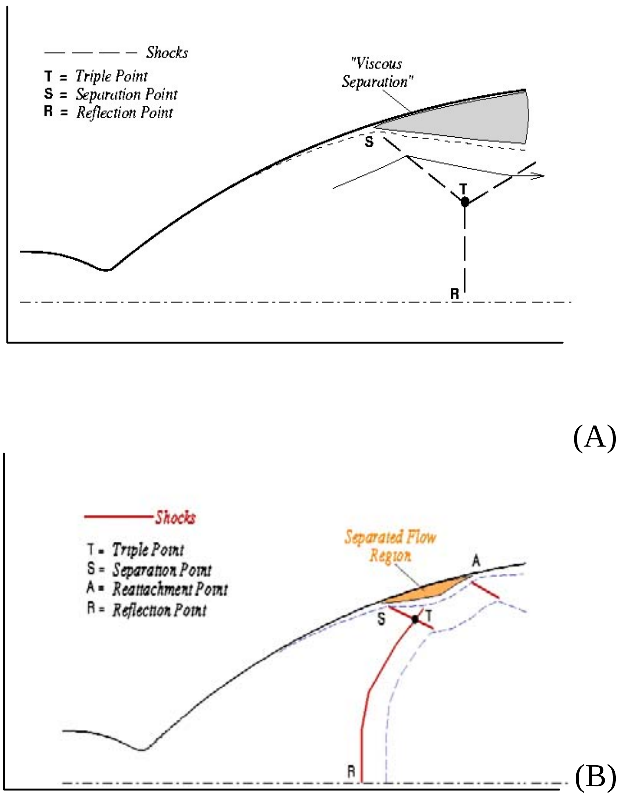

Fig. 1. Free (A) and Restricted (B) Shock Separation regimes

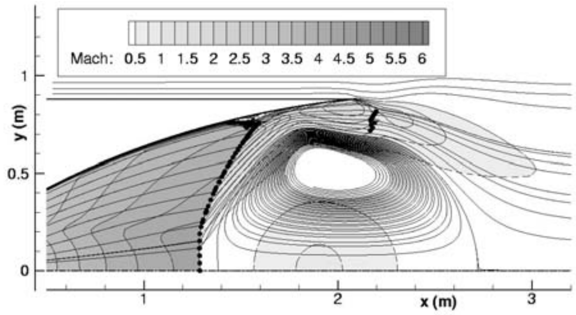

Fig. 2. The role of the centreline vortex in generating Restricted Shock Separation regimes

The Numerical Test Campaign

2.

2.1 Test Cases description

In order to give an answer on the above issues, a numerical campaign has been carried out. Main goals of the tests were:

- To understand the relationship between the curvature of the stem of the separation shock and the generation of the bubble of recirculating flow behind the shock,
- To find indications about the viscous or inviscid character of the phenomenon,

The flow domain considered is schematized in Fig. 3. It represents the overexpanded jet flow exhausting from a nozzle divergent section in a quiescent ambient with higher pressure. An oblique recompression shock takes place from the nozzle lip and is reflected at the nozzle axis, generating a Mach reflection shape. The flow is generated by the divergent section nozzle of the S6 TIC nozzle described in [11].

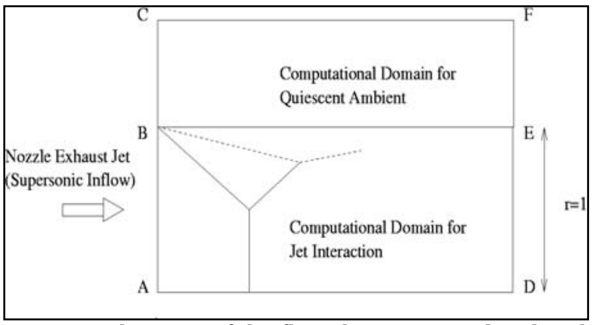

Fig. 3 . Schematic of the flow domain considered in the tests.

The following tests have been carried out:

1. Incoming inviscid flow, fully uniform.
2. Incoming overexpanded nozzle flow at different expansion levels (i.e. different non-uniformity levels in radial direction).
3. Same than 2), but viscous.

The numerical simulations have been performed by using the commercial CFD software package CFD++ developed by Metacomp Technologies, Inc..

2.2 Numerical results

<u>Test 1: Uniform jet.</u>
The incoming flow is a fully uniform supersonic stream. Its Mach number is M_i = 3.75 and the value of the ambient pressure is larger than the incoming value (p_a/p_i = 5.4). These features correspond to the exit average value of a flow of an ideal overexpanded nozzle designed at PR_d=108 and operating at PR=20.

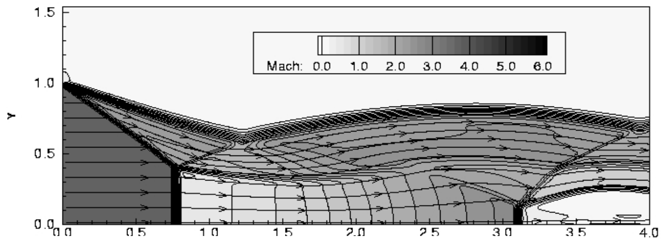

Fig. 4. Inviscid simulation with uniform incoming flow and classical Mach reflection

The computed flow field is shown in Fig. 4 by the Mach contour lines. Because of the uniform incoming stream, the shock reflection features the classical Mach reflection structure, with incident oblique shock, nearly-normal Mach stem and oblique reflected shock. The uniform distribution of the flow entering the shock also yields a subsonic flow behind the Mach stem, with a weak velocity component towards the nozzle axis near the triple point.

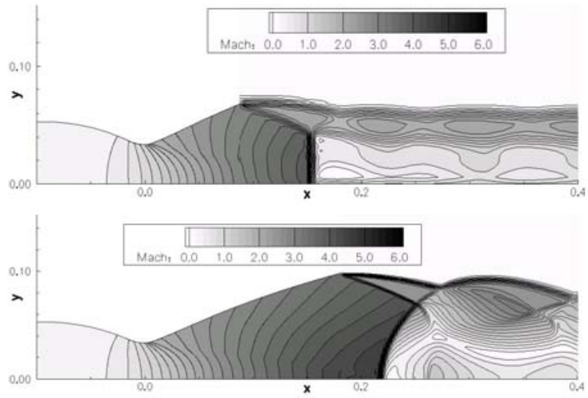

Fig. 5. Inviscid simulations with flat and curved Mach stem. (a) PR=10, (b) PR=20

Test 2: Jet from TIC nozzle

This second test concerns the exhaust flow of an overexpanded TIC nozzle at different expansion levels. Inviscid simulations have been carried out at different PR, cutting the nozzle at the separation position indicated by the experimental data [11] and simulating an overexpanded jet exhausting in a still ambient. In this case the flowfield is similar to the one generated by separation in steady-state overexpanded operations of the S6 TIC nozzle, at different PR.

The exhaust jet at the nozzle exit features different levels of non uniformity in radial direction, according to the PR considered. Fig. 5a indicate that at PR=10 the oblique shock generates a Mach reflection with a flat stem, quite similar to that obtained in Test 1, except a slight flow non-uniformity downstream of the shock. On the contrary, Fig. 5b indicates that at PR=20, when the radial flow gradients are stronger than PR=10, the oblique shock features a Mach reflection with a curved stem.

Although at PR=20 the average Mach number at the separation cross section is M=3.75, like in test case 1, the Mach stem is no longer flat, but rather curved. Indeed, the radial flow gradients leads to a substantially different Mach reflection structure. Moreover, because of the Mach stem curvature, the flowfield behind the shock features a large recirculating region (Fig. 5a).

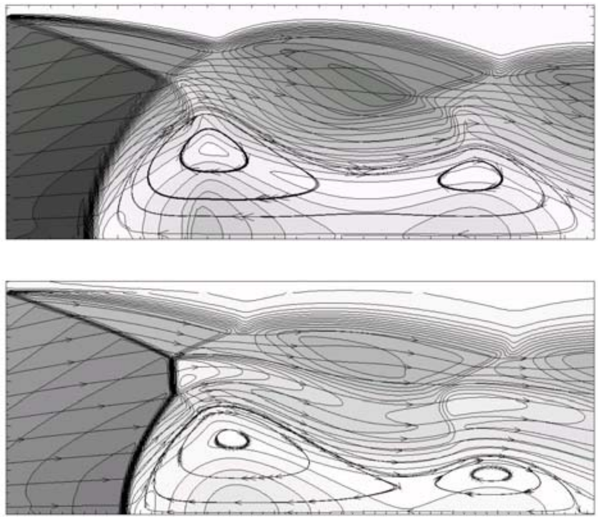

Fig. 6. Comparisons of viscous and inviscid results: (a) Inviscid flow, (b) Viscous laminar flow

Test 3: Viscous jet from TIC nozzle

The inviscid and viscous laminar flow solutions are similar. Figure 6a shows the flowfield obtained by an inviscid solution, whereas Fig. 6b is the solution of the same test in case of viscous laminar flow. Nevertheless, it is worth to refer that Ref. [12,13] have shown that in case of viscous turbulent flow, although the overall flow structure is still qualitatively similar to the inviscid case, the solution shows flatter Mach stem and smaller vortex. The implication of this effect for practical applications has still to be well analyzed at this stage.

Based on the comparisons of the above tests and other results available [13], the following conclusions have been reached:

i) both the solutions with flat or curved stems are different forms of Mach reflection of the oblique separation shock;
ii) despite of the absence of viscosity, the nozzle flow can be characterized by a curved shock profile and possibly by a flow recirculating region behind;
iii) a curved Mach stem can be generated also in TIC nozzles, independently of the oblique internal shock, typical of parabolic nozzles.

iv) The viscosity plays a secondary role in the generation of the nozzle flow structure, although turbulence reduces the shock curvature and thus the vortex dimension with respect to the inviscid and viscous-laminar solutions.

3. Flat or Curved Shock Shape

The different profiles of the reflection of the separation shock on the axis, can be explained by analyzing the characteristic line net in the nozzle divergent section, shown in Fig. 7.

In fact, in a TIC nozzle flow three regions of characteristic lines can be identified. The region I is the kernel, a "two-families" zone, where the expansion fans emanating from opposite sides of the throat interact each other. The combined effect of both families of characteristic waves on the expansion yields a nearly uniform flow in radial direction (Fig. 7b). The region II is a simple-wave region, and for two-dimensional ideal nozzles can be identified as a “one family” region of straight characteristic lines. In the axisymmetric case it is no longer a simple wave region, however the flow behavior is quite similar, as shown in Fig. 7a by the family of nearly-straight C+ characteristic lines. This region features the highest radial flow gradient, as clearly shown by the behaviour of the Mach contours in Fig. 7b.

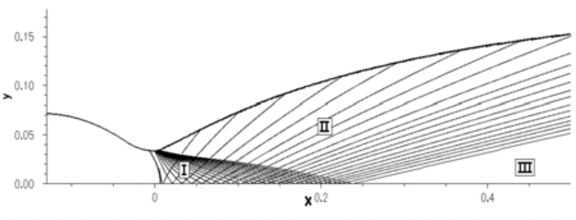

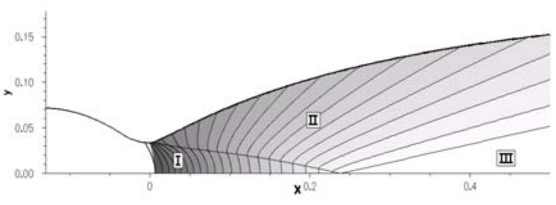

Fig. 7. Flow regions in a TIC nozzle: (a) Characteristic net, (b) Mach number isolines

Finally, region III is the fully uniform region.

On the basis of the above schematic it is possible to make an analytical reconstruction of the shape of the stem of any recompression shock located inside the nozzle divergent section.

The reconstruction is made on the basis of the inviscid solution of the nozzle flowfield. In particular, at each selected point along the nozzle axis where the recompression shock may be located, the Rankine-Hugoniot relationships can be applied to provide the pressure value downstream the shock, that can be assumed as a constant in the whole subsonic region downstream of the shock.

The shock shape can be reconstructed considering that because of the radial gradients of the flow incoming on the shock, the assumed downstream pressure value can only be matched by a shock of decreasing intensity. A possible solution is therefore a shock of changing slope, and, in the present case, a shock of increasing slope as the distance from axis increases. The shock shapes computed by the above method are shown in Fig. 8, along with the Mach number contour lines and the characteristic lines bounding the three different regions illustrated in Fig. 7.

Flat profiles are possibile when the shock is located either within the kernel of the characteristic net, or well inside the uniform flow zone. On the contrary, when the shock mainly lies in the non uniform region the shock shape features a curved profile. Cause of the “curved shock” structure is therefore the flow non uniformity.

Figure 8 clearly shows that at the abscissas where the extension of the kernel is dominant on the nozzle section, the upstream flow is nearly-uniform, and the shock features a quite flat shape. On the contrary, at the abscissas where region II occupies most of the nozzle cross section, the upstream flow is no longer uniform, and a curved shock shape takes place as shock profile. Finally, at the abscissas where a significant part of the nozzle section features a uniform flow the shock shape displays again a large flat vertical profile.

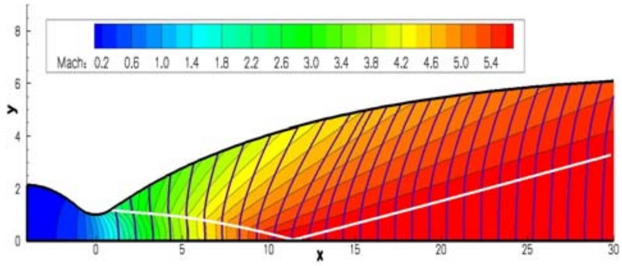

Fig. 8. Approximated shock profile reconstruction in a TIC nozzle

During a nozzle start-up for increasing nozzle PR a separation shock will move downstream along the axis, as well as the foot of its Mach stem. Therefore, there will be always a range of PR such that the Mach stem assumes a curved shape. In the region where the shock slope is clearly curved and only a small fraction of the shock stem lies in regions I or III, it can be expected that the shock profile is curved and a vortex will appear behind the shock, triggered by the radial flow gradients.
The different shock shapes shown in Fig. 5 can be explained on the basis of the above three flow regions. Indeed, in the first case with PR=10 (Fig. 5a), the Mach stem mainly lies in the region I, where only mild radial flow gradients take place: that yields a flat shape shock. In the second case with PR=20 (Fig. 5b) the Mach stem mainly lies in the region II, where stronger radial gradients prevail: thus it results in a curved shock shape.

4. Engineering model for the shock shape

On the basis of the findings of the above analysis and taking advantage of the inviscid nature of the phenomenon, an engineering model has been developed, capable of predicting location and shape of the separation shock and to provide indication about the possible generation of vortices behind the shock, in the core flow of the nozzle divergent section.

The numerical procedure has been illustrated with details in [13]. It is based on analytical relationships to evaluate the separation point, and on an empirical identification of the location of the triple point of the Mach reflection. To compute the shock shape a simple iterative scheme is adopted.

The prediction of the shock shape obtained by implementing the analytical model at PR=10, 14, and 20 is shown in Fig. 9, where it can be compared with the Mach number contours obtained by the relevant numerical solutions.

The engineering prediction can be considered in good agreement with the numerical solution, as it always shows a displacement lower than 5%. In particular, the predicted shock shape in the case of PR=20, displays a curved shock that generates a large bubble behind. The prediction is qualitatively similar to that provided by the numerical solution, although slightly displaced downstream. On the contrary the results of PR=10 and PR=14 show a slight shock curvature, such that the shock can be considered practically flat.

The differences between numerical solutions and prediction of the shock shape can be mainly explained by the constant pressure assumption in the region behind the shock. Indeed the numerical solution indicates a pressure variation behind the shock, providing a shock equilibrium profile less curved than that obtained by the assumption of a fully constant pressure.

5. Conclusion

The study on the origin of vortices that may take place during the overexpanded operation of rocket nozzles, indicates that their occurrence depends on the separation shock shape. Therefore, the basic characteristics of the flow separation in overexpanded nozzles and the physical origin of the separation shock shape have been analyzed.

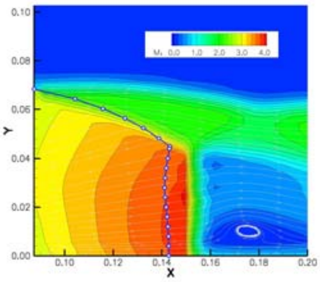

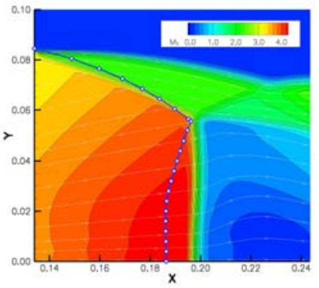

(a) (b)

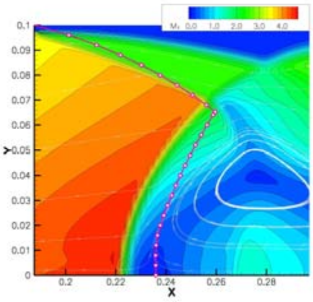

(c)

Figure 9. Analytical and numerical predictions of the shock shape for a separated TIC nozzle flow: Lines with circles=prediction; Mach number iso-contour and streamlines = numerical solution. (a) PR=10., (b) PR=14., (c) PR=20.

The numerical tests have shown that the driving factor is represented by the characteristics of the Mach reflection of the separation shock. In fact, the Mach reflection features flat or curved shape of the shock stem, depending on the location of the shock in a more or less uniform nozzle flow region.

In particular, the solutions show flat Mach stems when most of the shock lies in the kernel or the uniform flow region, and curved Mach stems when most of the shock lies in the "one-family" region of the characteristic net, located between the kernel and the uniform flow region.

The curved stem may yield downstream radial gradients in the core flow of the divergent section, that may generate a bubble of recirculating flow. The existence of this blockage is the necessary cause to shift from "free" to "restricted" flow separation regime.

Based on the findings of the above phenomenon, a simple analytical model has been developed that allows the prediction of location and shape of the stem of the Mach reflection of the separation shock. Its implementation to the nozzle considered has shown a good agreement with the numerical solution, with less than 5% displacements compared to the CFD solution.

Therefore, by a simple inviscid computation the model provides a first quick information on the stem curvature and thus on the possibility that vortices are generated behind the shock. The existence of these vortices indicates if it can be expected a possible transition from FSS to RSS, and therefore possible large side loads generation.

Acknowledgement

The present study was partially supported by MIUR (Italian Ministry of Education, University & Research).

References

[1] Nave, L. and Coffey, G., "Sea level side loads in High-Area-Ratio Rocket Engines," AIAA Paper 731284, Nov. 1973, 9th AIAA/SAE Propulsion Confer.

[2] Chen, C., Chakravarthy, S., and Hung, C., "Numerical Investigation of Separated Nozzle Flows," AIAA Journal, Vol. 32, No. 9, Sept. 1994.

[3] Nasuti, F. and Onofri, M., "Viscous and Inviscid Vortex Generation During Nozzle Flow Transients," AIAA Paper 96-0076, Jan. 1996, Also: AIAA Journal, Vol. 36, No. 5, May 1998.

[4] Frey, M., Stark, R., Ciezki, H. K., Quessard, F., and Kwan, W., "Subscale Nozzle Testing at the P6.2 Nozzle Stand," AIAA Paper 20003777, July 2000.

[5] Frey, M. and Hagemann, G., "Status of Flow Separation Prediction in Rocket Nozzles," AIAA Paper 98-3619, July 1998.

[6] Kwan, W. and Stark, R., "Flow Separation Phenomena in Subscale Rocket Nozzles," AIAA Paper 2002-4229, July 2002.

[7] Reijasse, P., Servel, P., and Hallard, R., "Synthesis of the 1998-99, ONERA Works in the FSCD Working Group," Tech.Rep. RTS 49/4361 DAFE/Y, ONERA, Chatillon Cedex, France, Dec. 1999.

[8] Girard, S. and Alziary de Roquefort, T., "Study of Flow Separation in Overexpanded Rocket Nozzles," 4th French-Russian-Italian-Uzbeck Workshop, Marseille, France, July 1997.

[9] Deck, S. and Guillen, P., "Numerical Simulation of Side Loads in Ideal Truncated Nozzle", Journal of Prop. and Power , Vol. 18, No. 2, 2002.

[10] Onofri, M. and Nasuti, F., "The Physical Origin of Side Loads in Rocket Nozzles" AIAA Paper 99--2587, July 1999.

[11] Ostlund, J., Flow processes in rocket engine nozzles with focus on flow separation and side loads, Royal Institute of Technology Department of Mechanics, Stockholm, Sweden, 2002.

[12] Nasuti, F., Onofri, M., and Pietropaoli, E.,"The Influence of Nozzle Shape on the Shock Structure in Separated Flows", ESA SP-563, Koln, November 2004.

[13] Nasuti, F., Onofri, M., and Pietropaoli, E., "Prediction of Shock Generated Vortices in Rocket Nozzles", AIAA Paper 2005-0317, Reno, 2005.